CREEP-FATIGUE CAVITIES AND THEIR TRANSITION TO SMALL CRACKS ALONG GRAIN BOUNDARIES IN TYPE 304 STAINLESS STEEL

N. TADA, T. KITAMURA, R. OHTANI and T. FUKUTA

Department of Engineering Physics and Mechanics, Graduate School of Engineering, Kyoto University, Kyoto, 606-01, JAPAN

ABSTRACT

Creep-fatigue tests of Type 304 stainless steel were carried out using smooth bar specimens. Cavities, which were initiated on grain boundaries inside the specimens, were observed on the cross-section by means of a scanning laser microscope. The results obtained are summarized as follows. In the very early stage of fatigue life, spherical cavities, the radius of which is less than 3μm, are randomly initiated on grain boundaries one after another. The only cavities that exist on grain boundaries perpendicular to the stress axis direction preferentially grow and change the shape from spherical to oblate (or crack-like). The initiation of a crack on each grain boundary, namely, a complete break of one grain boundary is brought about by immediate growth and coalescence of cavities when the reduction in area on the grain boundary reaches 0.5, which can be recognized as a condition of crack initiation on grain boundaries.

KEYWORDS

Creep-fatigue, cavity, crack initiation, grain boundaries, Type 304 stainless steel

INTRODUCTION

Under creep-dominant conditions, multiple cavities are initiated on grain boundaries in the very early stage of the fatigue life as a sign of the beginning of fracture, and their growth and coalescence bring about the initiation of small intergranular cracks, the size of which is about one grain boundary (Ohtani *et al.*, 1994, 1995; Kitamura *et al.*, 1995). In this paper, creep-fatigue test is carried out using smooth bar specimens of Type 304 stainless steel, and cavities, which are initiated inside the specimen, are observed on the cross-section of the specimens by means of a laser scanning microscope. The distribution of the size and shape of cavities are measured at different fatigue cycles, and a condition of crack initiation is discussed.

TEST CONDITION

Creep-fatigue test of Type 304 stainless steel were carried out at 1073K under total strain control using an electro-hydraulic testing machine equipped with a high-frequency induction

Table 1 Chemical composition of Type 304 stainless steel.

(wt.%)

C	Si	Mn	P	S	Cu	Ni	Cr	Mo	Fe
0.06	0.31	1.07	0.31	0.018	0.44	8.68	18.37	0.25	bal.

heating. Chemical composition of the material used and the shape of the specimen are shown in Table 1 and Fig.1, respectively. Strain waveform was slow tension-fast compression as shown in Fig.2. Under this condition, multiple cavities were initiated inside the specimens in the very early stage of fatigue life. The fatigue life was 133 cycles.

METHOD OF OBSERVATION

The creep-fatigue test was interrupted at different fatigue cycles, N/N_f=1/10, 1/6, 1/4 and 1/2. Namely, four interrupted specimens were prepared for the observation of cavities. In this paper, attention is paid to the behavior of cavities in the early and middle stages of fatigue life. Failure process in the latter stage including the propagation and coalescence of small cracks has already been reported (Zhou *et al.*, 1995).

Observation of cavities was carried out as follows. Firstly, the interrupted specimen was cut in the longitudinal direction at the center. The cross-section was polished with emery paper and was buffed up with diamond paste of about 1μm grains. A replica film of acetylcellulose was adhered and removed on the cross-section five times so as to clean the cross-section. A scanning laser microscope was used for the observation of cavities and area for cavity observation is shown in Table 2. The area varies depending on the number of cavities on the cross-section so as to obtain statistically valid results.

DISTRIBUTION OF CAVITIES ON GRAIN BOUNDARIES

Figure 3 shows photographs of cavities taken by a scanning laser microscope at N/N_f=1/2. Small cavities are initiated on grain boundaries and precipitates are also found there. The precipitates were found to be carbides by means of an electron probe microanalyzer. Interfacial fracture between carbides and matrix is thought to bring about the initiation of cavities.

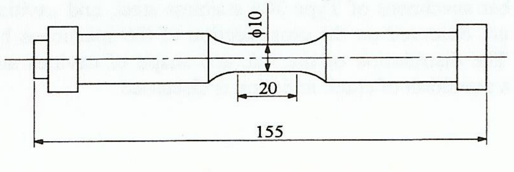

Fig.1 A smooth bar specimen for creep-fatigue test.

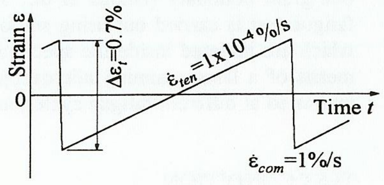

Fig.2 Strain waveform of slow-fast type.

Table 2 Area for cavity observation.

Life fraction, N/N_f	Observation area, S (mm^2)
1/10	4.43
1/6	3.11
1/4	1.83
1/2	1.19

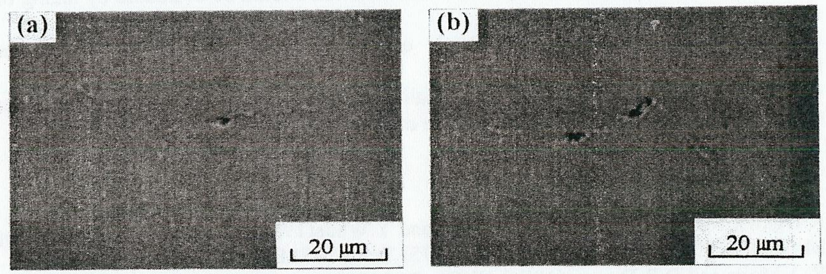

Fig.3 Cavities on grain boundaries observed by a scanning laser microscope.

Areal cavity density M, which is defined as the number of cavities in a unit area on the cross-section, is shown in Fig.4. As is found from Fig.4, cavities are initiated continuously from the very early stage of life. Grain boundary damage due to cavities increases with the number of fatigue cycles.

In order to evaluate the shape of cavities, each cavity is approximated by an ellipse, as shown in Fig.5, where a_c and h_c are the lengths in the grain boundary direction and in the direction perpendicular to the grain boundary direction, respectively, and θ_g is the angle of a grain boundary, which is defined as the angle of a linearized grain boundary (*i.e.*, a straight line between two triple points) against a line perpendicular to the stress axis, as shown in Fig.6. By means of a scanning laser microscope, the lengths of an object in two perpendicular directions

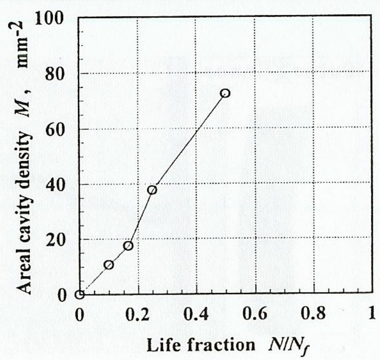

Fig.4 Change in areal cavity density, M, with life fraction, N/N_f.

such as those indicated by $2x_0$ and $2y_0$ in Fig.5, can be measured. Thus, a_c and h_c were calculated from θ_g, x_0 and y_0 by the following equations,

$$a_c = \sqrt{\frac{x_0^2 \cos^2\theta_g - y_0^2 \sin^2\theta_g}{\cos 2\theta_g}}, \qquad \left(0 \le \theta_g \le \pi/8,\ 3\pi/8 < \theta_g \le \pi/2\right) \tag{1}$$

$$h_c = \sqrt{\frac{y_0^2 \cos^2\theta_g - x_0^2 \sin^2\theta_g}{\cos 2\theta_g}}. \qquad \left(0 \le \theta_g \le \pi/8,\ 3\pi/8 < \theta_g \le \pi/2\right) \tag{2}$$

In the same manner, grain boundary angle, θ_g, is calculated by

$$\theta_g = \tan^{-1}\left(\frac{l_y}{l_x}\right), \quad \left(0 \le \theta_g \le \pi/2\right) \tag{3}$$

where l_x and l_y are the lengths in the direction perpendicular to the stress axis and in the stress axis direction, respectively.

Since eqs.(1) and (2) produce a relatively large error when the grain boundary angle, θ_g, is in the vicinity of $\pi/4$, a_c and h_c were calculated by

$$a_c = \sqrt{\frac{x_{45}^2 \cos^2\left(\theta_g - \frac{\pi}{4}\right) - y_{45}^2 \sin^2\left(\theta_g - \frac{\pi}{4}\right)}{\cos 2\left(\theta_g - \frac{\pi}{4}\right)}}, \quad \left(\pi/8 < \theta_g \le 3\pi/8\right) \tag{4}$$

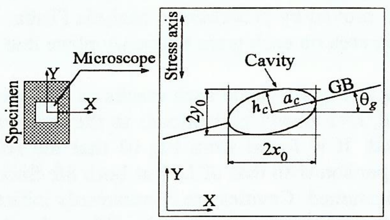

(a) When grain boundary angle, θ_g, is in the range of $0 \le \theta_g \le \pi/8$ or $3\pi/8 < \theta_g \le \pi/2$.

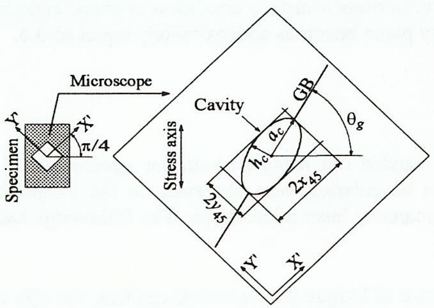

(b) When grain boundary angle, θ_g, is in the range of $\pi/8 < \theta_g \le 3\pi/8$.

Fig.5 A cavity approximated by an ellipse.

$$h_c = \sqrt{\frac{y_{45}^2 \cos^2\left(\theta_g - \frac{\pi}{4}\right) - x_{45}^2 \sin^2\left(\theta_g - \frac{\pi}{4}\right)}{\cos 2\left(\theta_g - \frac{\pi}{4}\right)}}. \quad \left(\pi/8 < \theta_g \le 3\pi/8\right) \tag{5}$$

using the lengths x_{45} and y_{45} in the case of $\pi/8 < \theta_g \le 3\pi/8$. x_{45} and y_{45} are the lengths which are measured by inclining the specimen by $\pi/4$(=45 degrees), as shown in Fig.5.

Figure 7 shows the relationship between the length and height of cavities. Until N/N_f=1/4, the size of cavities increases slowly but most of cavities are less than 3μm in length and height.

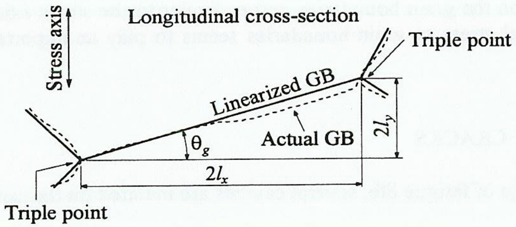

Fig.6 Angle of a grain boundary, θ_g.

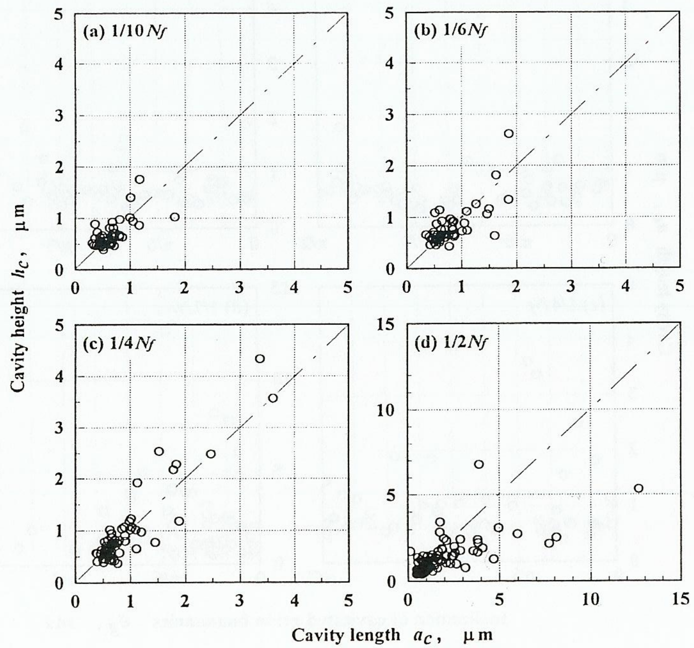

Fig.7 Correlation between the length and height of cavities.

Moreover, the fraction of h_c to a_c is almost unity. This means that the shape of cavities is spherical when the size is small. On the other hand, relatively large cavities are found at N/N_f=1/2 and their fraction of h_c to a_c is less than unity. The shape of cavities changes from spherical to oblate (or crack-like) as they grow.

Relationship between the inclination of cavitated grain boundaries (*i.e.*, grain boundaries on which cavities exist) and the length of cavities is shown in Fig.8. At N/N_f=1/10 and 1/6, the distribution of inclination of cavitated grain boundaries is almost uniform. Cavities are initiated independent of grain boundary angles against the stress axis. On the contrary, at N/N_f=1/4 and 1/2, larger cavities exist only on the grain boundaries which have lower value of θ_g. It is concluded that cavities are initiated independent of the grain boundary angle. However, such cavities as exist on the grain boundaries perpendicular to the stress axis direction, preferentially grow. The normal stress to grain boundaries seems to play an important roll in the growth of cavities.

INITIATION OF CRACKS

In the middle stage of fatigue life, several cavities are initiated on the same grain boundary and

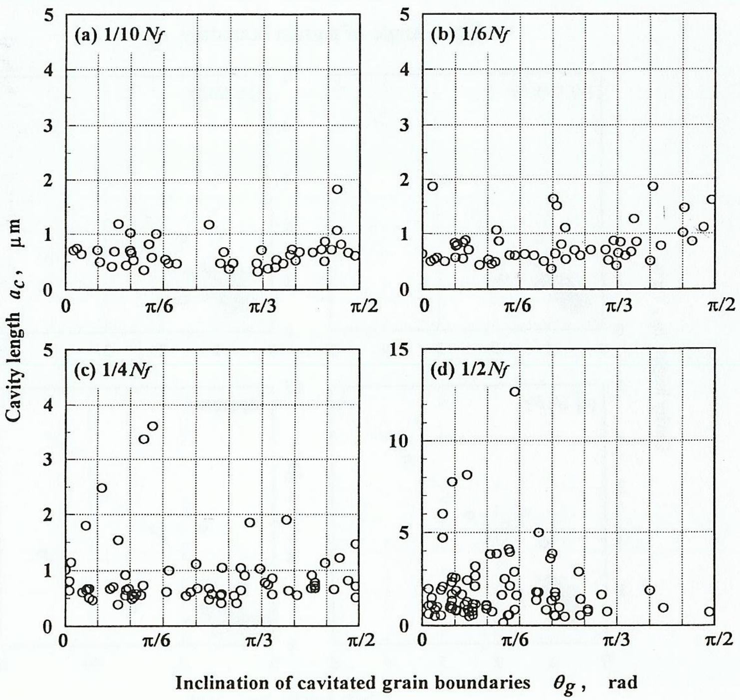

Fig.8 Correlation between the inclination of cavitated grain boundaries, θ_g, and cavity length, a_c.

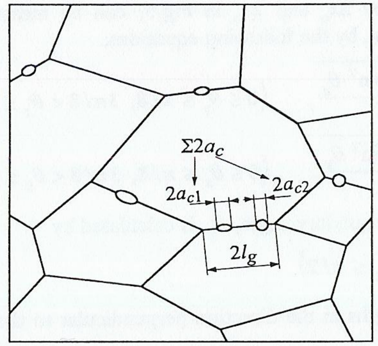

Fig.9 A schematic figure showing the fraction of cavities on grain boundary, L.

their growth and coalescence forms a crack of the size of one grain boundary. In this study, crack initiation is defined as a complete break of one grain boundary. In order to clarify a condition of crack initiation, fraction of cavities, L, which is schematically shown in Fig.9, is evaluated on each grain boundary at N/N_f=3/4 in addition to at N/N_f=1/2. L is given by

$$L = \frac{\sum 2a_i}{2l_g}, \tag{6}$$

where a_i and l_g are the length of cavities and that of the grain boundary on which the cavities exist, respectively. It has been proved by probabilistic analysis (Tada, 1996) that the value of L corresponds to the reduction in area on each grain boundary plane due to cavities.

The distribution of L is shown in Fig.10. Since such cracks as had grown to be larger than one grain boundary were not found, L=1 always corresponds to the case where a crack of the size of one grain boundary is initiated. It is found from Fig.10 that the relative frequency between L=0.5 and 0.9 is small in comparison with that of L=1 at both life fractions. Thus, the following process of crack initiation is presumed. Cavities are continuously initiated and grow slowly until a certain level of grain boundary damage (*i.e.*, L=0.5). When the damage reaches that level, growth and coalescence of cavities are highly accelerated and immediately forms a crack of the size of one grain boundary. In other words, a condition of crack initiation is that the reduction in area on the grain boundary plane becomes approximately equal to 0.5.

CONCLUSIONS

A creep-fatigue test was carried out using smooth bar specimens of Type 304 stainless steel. Cavities initiated on grain boundaries were observed on the longitudinal cross-section of the specimens by means of a scanning laser microscope. The followings were clarified in the present paper.

(1) From the very early stage of fatigue life, spherical cavities, the size of which is less than 3μm, are initiated on grain boundaries. The initiation is independent of the inclination of the grain boundary.

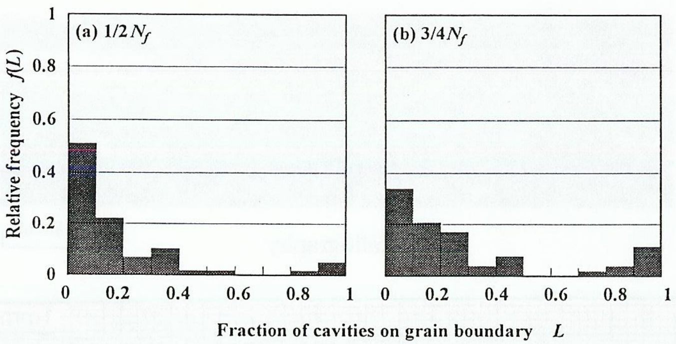

Fig. 10 Distribution of fraction of cavities on grain boundary, $f(L)$.

(2) Only the cavities that exist on the grain boundaries perpendicular to the stress axis direction preferentially grow. This suggests that the normal stress acting on the grain boundary plays an important roll in the growth of cavities.

(3) As cavities grow, their shape changes from spherical to oblate (crack-like).

(4) Relative frequency of fraction of cavities on each grain boundary, L, is small in the range from 0.5 to 0.9 in comparison with that of L=1 (*i.e.*, in the case of a complete break of the grain boundary). This suggests that the growth and coalescence of cavities take place immediately at the moment L reached 0.5. Considering that the fraction of cavities on the grain boundary corresponds to the reduction in area on the grain boundary plane, a condition of crack initiation is that the reduction in area on the grain boundary plane reaches 0.5.

REFERENCES

KITAMURA, T., R. OHTANI, N. TADA and W. ZHOU (1995). Characterization of creep-fatigue fracture of Type 304 stainless steel based on initiation and growth of small cracks. In: *Service Experience, Structural Integrity, Severe Accidents, and Erosion in Nuclear and Fossil Plants*, PVP Vol.303, pp. 377-382. ASME.
OHTANI, R., T. KITAMURA, N. TADA and W. ZHOW (1994). Experimental mechanics on initiation and growth of distributed small creep-fatigue cracks. In: Recent Advances in Experimental Mechanics (S. Gomes *et al.*, ed.), pp. 1173-1179. Balkema, Rotterdam.
OHTANI, R., T. KITAMURA and W. ZHOU (1995). Effect of internal creep microcracks on fatigue macrocrack propagation at high temperatures. *Mat. Sci. Res. Int.*, **1**, 238-246.
TADA, N., T. KITAMURA and R. OHTANI (1996). Physical meaning of creep damage parameters evaluated from distribution of grain boundary cavities on cross-section. *J. Soc. Mat. Sci. Japan*, **45**, 110-117 (in Japanese).
ZHOU, W., R. OHTANI, T. KITAMURA, N. TADA and A. KOSAKA (1995). Creep-fatigue intergranular fracture of inner cracking type in Type 304 stainless steel. *J. Soc. Mat. Sci. Japan*, **44**, 78-83 (in Japanese).